Deuterium Quadrupole Coupling Constants and Asymmetry Parameters in Bridging Metal Hydride Complexes

Ae Ja Kim,[1a] Frank R. Fronczek,[1a] Leslie G. Butler,*,†,[1a] Shixiong Chen,[1b] and Ellen A. Keiter*,[1b]

Contribution from the Department of Chemistry, Louisiana State University, Baton Rouge, Louisiana 70803-1804, and the Department of Chemistry, Eastern Illinois University, Charleston, Illinois, 61920. *Received April 8, 1991*

Abstract: The deuterium quadrupole coupling constants and the asymmetry parameters for six bridging metal hydrides, $[Et_4N][^2HCr_2(CO)_{10}]$, $[(Ph_3P)_2N][^2HCr_2(CO)_{10}]$, $[Ph_4P][^2HCr_2(CO)_{10}]$, $[Et_4N][^2HW_2(CO)_{10}]$, $[(Ph_3P)_2N][^2HW_2(CO)_{10}]$, and $[Ph_4P][^2HW_2(CO)_{10}]$, were determined from the Levenberg-Marquardt nonlinear least-squares fit of the solid-state deuterium NMR powder patterns. The quadrupole coupling constant (absolute value) varies from 54.1 (8) to 90.4 (2) kHz; the asymmetry parameter ranges from 0.027 (3) to 0.31 (2). The relationships between the quadrupole coupling constant and M-H bond length and between the asymmetry parameter and the M-H-M bond geometry are discussed on the basis of a point charge model. In order to assess motional averaging at the deuterium site, the temperature dependence of the ^2H NMR spectrum for two bridging metal hydrides was examined at 140, 200, and 300 K. In addition, the isotropic chemical shifts have been obtained from ^1H CRAMPS. These NMR results are highly pertinent to NMR spectroscopy of adsorbed hydrogen on metal surfaces. The solid-state structure of $[Ph_4P][^2HCr_2(CO)_{10}]$ has been determined by X-ray diffraction.

Introduction

The M-H-M bond in the $[HM_2(CO)_{10}]^-$ monoanion (M = Cr, Mo, W) has been of considerable interest because it contains a single unsupported three-center bond.[2-6] Unlike the linear hydrogen bonds found in KHF_2[7] and $Na[Me_3Al\text{-}H\text{-}AlMe_3]$,[8-10] the bridging metal hydride bonds in these transition-metal dimers are bent,[11-15] even when the metal carbonyl framework has a pseudo D_{4h} geometry, as shown in Figure 1a for $[Et_4N][HCr_2(CO)_{10}]$.[11] The metal carbonyl framework is sensitive to the counterion with a bent staggered geometry being relatively common,[3,4,11-15] as shown in Figure 1b. Metal hydrides are common species on surfaces and may often exist in a bridging environment.[16,17]

Solid-state deuterium NMR techniques have previously been used to characterize the terminal metal hydride sites in $(\eta_5\text{-}C_5H_5)_2Mo(^2H)_2$,[18] $(\eta_5\text{-}C_5H_5)_2W(^2H)_2$,[18] $(\eta_5\text{-}C_5H_5)_2Zr(^2H)_2$,[19] and $^2HMn(CO)_5$[20] and to determine the charge on a carbon atom in an organometallic alkyl complex.[21] Recently, dynamic information about the rotational jump motion for the cyclopentadienyl ring in $(\mu\text{-}CO)_2[FeCp(CO)]_2$ was obtained from deuterium line shape analyses and T_1 measurements.[22]

Deuterium quadrupole coupling constants have been measured in a wide variety of bridging hydrogen sites: K^2HF_2,[7,23] O-^{2}H···O in $CuSO_4\cdot 5H_2O$[24] and many other hydrogen bonds with oxygen atom donors and acceptors,[24-26] and N-^{2}H···O in anthranilic acid[27] and other systems involving nitrogen atom donors and/or acceptors.[28,29] Also, relatively accurate calculations can be made using ab initio molecular orbital techniques and extended basis sets. One possibility revealed by the results of calculations is that of a negative quadrupole coupling constant, either in a nonlinear site, as in diborane,[30-34] or for a particularly long, symmetric linear hydrogen bond.[25]

In this work we are trying to obtain structural information on the M-^{2}H-M unit in the $[^2HM_2(CO)_{10}]^-$ monoanion (M = Cr, W) by using solid-state deuterium NMR spectroscopy. This quest is based on the fact that the solid-state deuterium NMR spectrum of a powder is determined by two measurable parameters,[35] the quadrupole coupling constant and the asymmetry parameter, which describe the principal elements of the electric field gradient tensor.[36] The quadrupole coupling constant is a measure of the magnitude of the electric field gradient at the deuterium site, while the asymmetry parameter gives information about the shape of the electric field gradient; for example, an asymmetry parameter of zero suggests at least 3-fold symmetry at deuterium. Consequently, both parameters will be related to the M-H bond distance and the H-H-M bond angle.

* To whom correspondence should be addressed.
† Fellow of the Alfred P. Sloan Foundation (1989-1991).

(1) (a) Louisiana State University, (b) Eastern Illinois University.
(2) Handy, L. B.; Ruff, J. K.; Dahl, J. F. *J. Am. Chem. Soc.* **1970**, *92*, 7312-26.
(3) Bau, R.; Teller, R. G.; Kirtley, S. W.; Koetzle, T. F. *Acc. Chem. Res.* **1979**, *12*, 176-83.
(4) Hart, D. W.; Bau, R.; Koetzle, T. F. *Organometallics* **1985**, *4*, 1590-4.
(5) Harris, D. C.; Gray, H. B. *J. Am. Chem. Soc.* **1975**, *97*, 3073-5.
(6) Eyermann, C. J.; Chung-Phillips, A. *Inorg. Chem.* **1984**, *23*, 2025-9.
(7) Blinc, R.; Rutar, V.; Seliger, J.; Slak, J.; Smolej, V. *Chem. Phys. Lett.* **1977**, *48*, 576-8.
(8) Atwood, J. L.; Hrncir, D. C.; Rogers, R. D.; Howard, J. A. K. *J. Am. Chem. Soc.* **1981**, *103*, 6787-8.
(9) Howell, J. M.; Sapse, A. M.; Singman, E.; Snyder, G. *J. Am. Chem. Soc.* **1982**, *104*, 4758-9.
(10) Chiles, R. A.; Dykstra, C. E. *Chem. Phys. Lett.* **1982**, *92*, 471-3.
(11) Roziere, J.; Williams, J. M.; Stewart, R. P., Jr.; Petersen, J. L.; Dahl, L. F. *J. Am. Chem. Soc.* **1977**, *99*, 4497-9.
(12) Petersen, J. L.; Johnson, P. L.; O'Connor, J.; Dahl, L. F.; Williams, J. M. *Inorg. Chem.* **1978**, *17*, 3460-9.
(13) Bau, R.; Koetzle, T. F. *Pure Appl. Chem.* **1978**, *50*, 55-63.
(14) Petersen, J. L.; Brown, R. K.; Williams, J. M.; McMullan, R. K. *Inorg. Chem.* **1979**, *18*, 3493-8.
(15) Wilson, R. D.; Graham, S. A.; Bau, R. *J. Organometal. Chem.* **1975**, *91*, C49-52.
(16) Ertl, G. In *The Nature of the Surface Chemical Bond*; Rhodin, T. M., Ertl, G., Eds.; North-Holland: Amsterdam, 1979, Chapter 5.
(17) Panas, I.; Siegbahn, P. E. M. *J. Chem. Phys.* **1990**, *92*, 4625-7.
(18) Wei, I. Y.; Fung, B. M. *J. Chem. Phys.* **1971**, *55*, 1486-7.
(19) Jarrett, W. L.; Farlee, R. D.; Butler, L. G. *Inorg. Chem.* **1987**, *25*, 1381-3.
(20) Ireland, P. S.; Olson, L. W.; Brown, T. L. *J. Am. Chem. Soc.* **1975**, *97*, 3548-9.
(21) Altbach, M. I.; Hiyama, Y.; Gerson, D. J.; Butler, L. G. *J. Am. Chem. Soc.* **1987**, *109*, 5529-31.
(22) Altbach, M. I.; Hiyama, Y.; Wittebort, R. J.; Butler, L. G. *Inorg. Chem.* **1990**, *29*, 741-7.
(23) Dixon, M.; Overill, R. E.; Platt, E. *J. Mol. Struct.* **1978**, *48*, 115-122.
(24) Soda, G.; Chiba, T. *J. Chem. Phys.* **1969**, *50*, 439-55.
(25) Butler, L. G.; Brown, T. L. *J. Am. Chem. Soc.* **1981**, *103*, 6541-6549.
(26) Brown, T. L.; Butler, L. G.; Curtin, D. Y.; Hiyama, Y.; P., I. C.; Wilson, R. G. *J. Am. Chem. Soc.* **1982**, *104*, 1172-1177.
(27) d'Avignon, D. A.; Brown, T. L. *J. Phys. Chem.* **1981**, *85*, 4073-9.
(28) Keiter, E. A.; Hiyama, Y.; Brown, T. L. *J. Mol. Struct.* **1983**, *111*, 1-10.
(29) Hiyama, Y.; Keiter, E. A.; Brown, T. L. *J. Magn. Reson.* **1986**, *67*, 202-10.

0002-7863/91/1513-9090$02.50/0

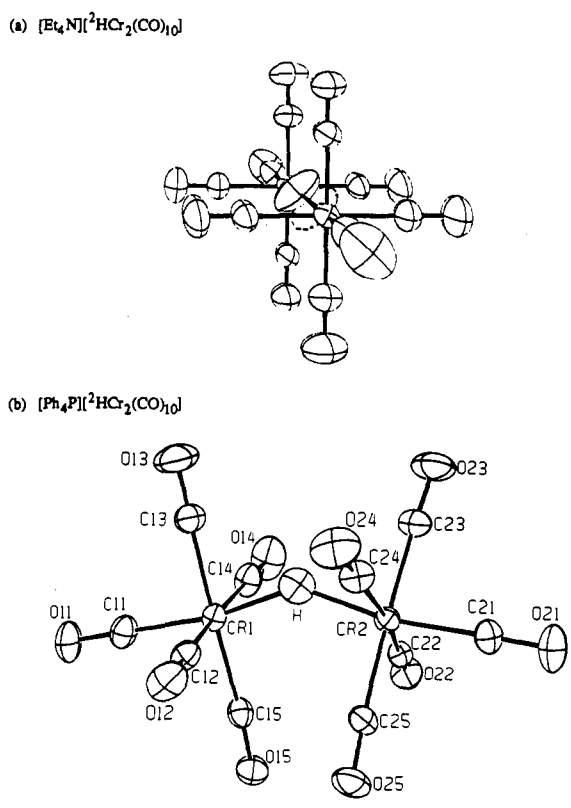

Figure 1. The flexible geometry of the M–H–M structure in the $[HM_2(CO)_{10}]^-$ anion is shown for two representative structures. (a) The metal carbonyl framework shown in an eclipsed configuration (from a neutron diffraction study of $[Et_4N][HCr_2(CO)_{10}]$, reprinted with permission from ref 11). The bridging hydride is crystallographically disordered; the Cr–H–Cr bond exhibits a bent structure. (b) The bent staggered metal–carbonyl geometry is shown here for the anion of $[Ph_4P][^2HCr_2(CO)_{10}]$ (this work).

Theory

For the calculation of the deuterium powder pattern NMR line shape, the total Hamiltonian is given by a combination of Zeeman and quadrupolar interactions

$$\mathcal{H}_{total} = -\gamma\mathcal{H}_0(1 + \sigma_{iso})I_z + \mathcal{H}_Q \qquad (1)$$

where γ is the gyromagnetic ratio for deuterium, $2\pi \times 653.5$ rad s^{-1} G^{-1}, H_0 is the applied magnetic field, I is the deuterium spin angular momentum operator in the laboratory coordinate system, and σ_{iso} is the isotropic chemical shift relative to TMS. The quadrupole coupling Hamiltonian for a nucleus with $I \geq 1$ is given by[35]

$$\mathcal{H}_Q = \frac{eQ/\hbar}{6I(2I-1)}\sum_{kj} V_{kj}^{lab}\left[\frac{3}{2}(I_kI_j + I_jI_k) - \delta_{kj}I^2\right] \qquad (2)$$

where Q is the nuclear quadrupole moment, 2.86×10^{-27} cm^2 for deuterium[37] and δ_{kj} is the kronecker delta. The electric field gradient, V_{kj} ($= eq_{kj}$), can be described as a symmetric 3×3 traceless tensor with the convention $|eq_{zz}| \geq |eq_{yy}| \geq |eq_{xx}|$.[36] The magnitude of the electric field gradient tensor is given by the quadrupole coupling constant, $e^2q_{zz}Q/h$. The deviation from axial symmetry is indicated by the asymmetry parameter, η:

$$\eta = \frac{eq_{yy} - eq_{xx}}{eq_{zz}} \qquad (0 \leq \eta \leq 1) \qquad (3)$$

In the principal axis system, the electric field gradient tensor can be reduced to two parameters, eq_{zz} and η:

$$V^{PA} = -\frac{eq_{zz}}{2}\begin{bmatrix} (I-\eta) & 0 & 0 \\ 0 & (I+\eta) & 0 \\ 0 & 0 & -2 \end{bmatrix} \qquad (4)$$

The transformation between the laboratory coordinate system (Lab) and the molecular coordinate system (PA) is accomplished with direction cosine matrices[38] using the y-convention:[39]

$$V^{Lab} = \mathbf{R}_N^{-1}(\theta)\mathbf{R}_z^{-1}(\chi)V^{PA}\mathbf{R}_z(\chi)\mathbf{R}_N(\theta) \qquad (5)$$

Only two Euler angles, θ and χ, are needed to orient the electric field gradient tensor relative to the applied magnetic field, $\mathcal{H}_0$.

The transition frequencies are obtained by solving the eigenvalue problem for $\mathcal{H}_{total}$ at a given orientation, θ and χ. There are two allowed transitions among the deuterium spin states: $|+1\rangle \rightarrow |0\rangle$ and $|0\rangle \rightarrow |-1\rangle$. Thus, the deuterium powder patterns are obtained by summing the deuterium transition frequencies over a range of θ and χ orientations within the limits of 0 and 90° with sin (θ) weighting.[40] Typically, we use a uniform step angle of 2°, and the calculation takes about 10 min on a VAXstation 3200. At the temperatures and the magnetic fields used here, the shape of the deuterium powder does not depend upon the sign of the quadrupole coupling constant, thus the sign cannot be determined. However, at extreme conditions, for example, 0.02 K and 18 T, Boltzmann statistics do affect the line shape such that the sign can be obtained, provided a small tip angle rf pulse is used.[41]

The elements of the electric field gradient tensor are the sum of nuclear and electronic terms, the latter is expressed as an expectation value of the electronic wave function Ψ,

$$eq_{zz} = +\sum_n K_n\frac{3z_n^2 - r_n^2}{r_n^5} - e\left\langle \Psi^*\left|\sum_i \frac{3z_i^2 - r_i^2}{r_i^5}\right|\Psi\right\rangle \qquad (6)$$

where e is the electronic charge, n is the index over the other nuclei whose charge is K_n, and i is the index over the electrons of the molecule. Molecular wave functions suitable for use in eq 6 can be obtained from ab initio SCF-HF calculations provided extended basis sets are used.[30-32] In the absence of detailed molecular wave functions, an approximate analysis is often feasible using point charges to represent the combined nuclear and electronic contributions from neighboring atoms. Thus, at the bridging deuteron, two point charges representing the metals will produce an electric field gradient along the z-axis (PA)

$$\frac{e^2q_{zz}Q}{h} = \left(\frac{e^2Q}{h}\right)(2K')\left(\frac{3z^2 - r^2}{r^5}\right) = \left(\frac{e^2Q}{h}\right)(2K')\left(\frac{3\sin^2(\theta/2) - 1}{r^3}\right) \qquad (7)$$

where r is the M–H bond length, θ is the M–H–M bond angle, and z is along the M···M vector. Analogous expressions apply for eq_{xx} and eq_{yy}. The adjustable parameter, K', was determined from the experimental quadrupole coupling constant for $[Et_4N][^2HCr_2(CO)_{10}]$ at 300 K and has a value of +1.104 e, with the assumption that the sign of the quadrupole coupling constant is positive.[42] Due to the $1/r^3$ distance dependence, charges close

(30) Huber, H. *J. Chem. Phys.* **1985**, *83*, 4591–8.
(31) Snyder, L. C.; Basch, H. *Molecular Wave Functions and Properties*; John Wiley & Sons: New York, 1972.
(32) Snyder, L. C. *J. Chem. Phys.* **1978**, *68*, 291–4.
(33) Barfield, M.; Gottlieb, H. P. W.; Doddrell, D. M. *J. Chem. Phys.* **1978**, *69*, 4504–15.
(34) Witschel, J., Jr.; Fung, B. M. *J. Chem. Phys.* **1972**, *56*, 5417–22.
(35) Gerstein, B. C.; Dybowski, C. R. *Transient Techniques in NMR of Solids*; Academic Press: New York, 1985.
(36) Poole, C. P.; Farach, H. A. *Theory of Magnetic Resonance*; Wiley-Interscience: New York, 1987.
(37) Reid, R. V., Jr.; Vaida, M. L. *Phys. Rev. Lett.* **1975**, *34*, 1064.
(38) Zare, R. N. *Angular Momentum*; Wiley-Interscience: New York, 1988.
(39) Goldstein, H. *Classical Mechanics*, 2nd ed.; Addison-Wesley: New York, 1980; note error in eq B-3y.
(40) A more efficient weighting scheme has been reported. Alderman, D. W.; Solum, M. S.; Grant, D. M. *J. Chem. Phys.* **1986**, *84*, 3717–25.
(41) Waugh, J. S.; Gonen, O.; Kuhns, P. *J. Chem. Phys.* **1987**, *86*, 3816–8.

Table I. Crystal, Experimental, and Refinement Data for $[Ph_4P][^2HCr_2(CO)_{10}]$

mol formula	$Cr_2PC_{34}H_{21}O_{10}$
fw	724.5
a, Å	14.2384 (9)
b, Å	16.6178 (12)
c, Å	15.9909 (8)
β, deg	115.511 (5)
V, Å^3	3414.7 (9)
Z	4
D_{calcd}, g cm^{-3}	1.409
λ, Å	0.71073
cryst syst	monoclinic
space group	$P2_1/c$
μ, cm^{-1}	7.2
cryst dimens, mm	0.10 × 0.12 × 0.50
color	yellow
min rel transmissn, %	93.84
temp, °C	26
scan type	ω–2θ
θ limits, deg	1–25
no. of reflcns	5988
no. of obsd reflcns	4268
observn criterion	$I > 1\sigma(I)$
no. of params refined	428
$R = \sum\|\Delta F\|/\sum F_o$	0.055
$R_w = (\sum w(\Delta F)^2/\sum wF^2)^{1/2}$	0.043
max resid density, e Å^{-3}	0.33
min resid density, e Å^{-3}	−0.34

to the origin have the greatest effect on the electric field gradient. With this model, the effects of structural variations in a static nonlinear bridging metal hydride on the values of the quadrupole coupling constant and the asymmetry parameter can be assessed, as shown in Figure 2. Early on, a deficiency in the point charge model was found; an exaggerated dependence of the symmetry parameter on the bond angle is apparent on comparison with the experimental results. Therefore, also shown in Figure 2b are the results from a set of ab initio molecular orbital calculations for a model system, $[Na–H–Na]^+$.[43]

Experimental Methods

Sample Preparation. Bridging metal hydrides, $[Et_4N][HCr_2(CO)_{10}]$, $[(Ph_3P)_2N][HCr_2(CO)_{10}]$, $[Ph_4P][HCr_2(CO)_{10}]$, $[Et_4N][HW_2(CO)_{10}]$, $[(Ph_3P)_2N][HW_2(CO)_{10}]$, and $[Ph_4P][HW_2(CO)_{10}]$, were synthesized from $Cr(CO)_6$ or $W(CO)_6$ and $NaBH_4$ according to the method described by Hayter for the tetraethylammonium salt.[44] For preparation of the bis(triphenylphosphine)iminium and tetraphenylphosphonium salts, $[(Ph_3P)_2N]Cl$ and $[Ph_4P]Cl$ were substituted for $[Et_4N]Br$. Identical methods were utilized for preparing the deuterated complexes except that $NaBD_4$ was used as the reducing agent. All reactants were reagent grade and were used as obtained from commercial sources without further purification. Purity of products was established by infrared spectroscopy. In cases where spectra of the initial product showed evidence of contamination by $M(CO)_6$, recrystallization from either ethanol or tetrahydrofuran/hexane was effected until all infrared evidence of starting material had been eliminated. Solution ^1H NMR data were recorded with a Varian T-60 spectrometer in deuteroacetone solutions.

Crystallographic Work for $[Ph_4P][^2HCr_2(CO)_{10}]$. Diffraction data were collected on an Enraf-Nonius CAD4 diffractometer equipped with Mo Kα radiation and a graphite monochromator. Data reduction included corrections for Lorentz, polarization, background, and absorption effects. Absorption corrections were based on Ψ scans. The structure was refined by full-matrix least squares based on F. Calculations using the Enraf-Nonius SDP programs.[45] Non-hydrogen atoms were refined anisotropically; the bridging hydride was refined isotropically, while hydrogens bound to carbon were placed in calculated positions. Crystal, experimental, and refinement data are given in Table I. Atomic positions are listed in Table II. Selected bond distances and bond angles are listed in Table III. Figure 1b shows the atom-labeling scheme for the $[^2HCr_2(CO)_{10}]^-$ anion in $[Ph_4P][^2HCr_2(CO)_{10}]$.

(42) $e^2q_{zz}Q/h$ = +85.4 kHz, $r = 1.7 \times 10^{-8}$ cm, θ = 158.9°.
(43) Guo, K.; Jarrett, W. L.; Butler, L. G. *Inorg. Chem.* **1987**, *26*, 3001–4.
(44) Hayter, R. G. *J. Am. Chem. Soc.* **1966**, *88*, 4376–82.
(45) Frenz, B. A. *Enraf Nonius Structure Determination Package SDP/VAX V3.0*; Enraf-Nonius: Delft, Holland, copyright 1985.

Table II. Coordinates and Equivalent Isotropic Thermal Parameters for $[Ph_4P][^2HCr_2(CO)_{10}]$

atom	x	y	z	B_{eq},[a] Å^2
Cr1	0.20618 (4)	0.56338 (4)	0.57651 (4)	4.14 (1)
Cr2	0.42548 (4)	0.46794 (4)	0.67861 (4)	3.90 (1)
C11	0.0905 (3)	0.6223 (3)	0.5051 (3)	5.6 (1)
O11	0.0187 (2)	0.6603 (2)	0.4597 (2)	8.1 (1)
C12	0.1579 (3)	0.4726 (2)	0.4994 (3)	5.2 (1)
O12	0.1287 (2)	0.4179 (2)	0.4526 (2)	8.19 (9)
C13	0.1440 (3)	0.5234 (3)	0.6524 (3)	6.1 (1)
O13	0.1088 (2)	0.5004 (3)	0.6984 (2)	10.6 (1)
C14	0.2652 (3)	0.6486 (3)	0.6607 (3)	5.9 (1)
O14	0.3008 (3)	0.6994 (2)	0.7121 (2)	9.3 (1)
C15	0.2714 (3)	0.6007 (2)	0.5029 (3)	4.7 (1)
O15	0.3061 (2)	0.6247 (2)	0.4558 (2)	6.69 (8)
C21	0.5509 (3)	0.4157 (2)	0.7196 (3)	5.3 (1)
O21	0.6300 (2)	0.3837 (2)	0.7443 (2)	8.4 (1)
C22	0.4808 (3)	0.5701 (2)	0.6760 (2)	4.23 (9)
O22	0.5130 (2)	0.6331 (2)	0.6755 (2)	6.09 (8)
C23	0.4503 (3)	0.4869 (3)	0.8024 (3)	5.4 (1)
O23	0.4683 (3)	0.4976 (2)	0.8780 (2)	9.0 (1)
C24	0.3499 (3)	0.3746 (3)	0.6770 (3)	5.9 (1)
O24	0.3016 (3)	0.3193 (2)	0.6752 (2)	9.3 (1)
C25	0.4062 (3)	0.4490 (2)	0.5554 (2)	4.7 (1)
O25	0.3988 (2)	0.4363 (2)	0.4833 (2)	7.38 (9)
P	0.18883 (6)	0.40053 (6)	−0.00915 (6)	3.29 (2)
C31	0.2968 (2)	0.3435 (2)	−0.0067 (2)	3.36 (8)
C32	0.3772 (3)	0.3217 (2)	0.0768 (2)	4.6 (1)
C33	0.4610 (3)	0.2788 (2)	0.0771 (3)	5.6 (1)
C34	0.4629 (3)	0.2570 (3)	−0.0042 (3)	6.2 (1)
C35	0.3836 (3)	0.2781 (3)	−0.0872 (3)	6.3 (1)
C36	0.2995 (3)	0.3214 (2)	−0.0892 (3)	5.0 (1)
C41	0.2082 (3)	0.5054 (2)	−0.0217 (2)	3.72 (9)
C42	0.2816 (3)	0.5299 (3)	−0.0506 (3)	5.9 (1)
C43	0.2966 (4)	0.6112 (3)	−0.0586 (3)	8.7 (2)
C44	0.2414 (4)	0.6667 (3)	−0.0348 (4)	8.6 (2)
C45	0.1707 (4)	0.6423 (3)	−0.0052 (4)	7.7 (2)
C46	0.1526 (3)	0.5623 (3)	0.0009 (3)	6.1 (1)
C51	0.0724 (2)	0.3651 (2)	−0.1036 (2)	3.36 (8)
C52	0.0007 (3)	0.4180 (2)	−0.1643 (3)	4.9 (1)
C53	−0.0911 (3)	0.3879 (3)	−0.2328 (3)	6.9 (1)
C54	−0.1108 (3)	0.3072 (3)	−0.2405 (3)	6.4 (1)
C55	−0.0391 (3)	0.2549 (3)	−0.1817 (3)	5.4 (1)
C56	0.0530 (3)	0.2827 (2)	−0.1132 (2)	4.13 (9)
C61	0.1789 (2)	0.3878 (2)	0.0983 (2)	3.45 (8)
C62	0.1157 (3)	0.3296 (3)	0.1079 (2)	5.1 (1)
C63	0.1145 (3)	0.3180 (3)	0.1932 (3)	7.2 (1)
C64	0.1737 (3)	0.3653 (3)	0.2666 (3)	6.5 (1)
C65	0.2372 (3)	0.4227 (3)	0.2580 (3)	6.2 (1)
C66	0.2392 (3)	0.4348 (3)	0.1735 (3)	5.3 (1)
H	0.305 (3)	0.507 (2)	0.658 (2)	8 (1)[b]

[a] The equivalent isotropic thermal parameter is defined by equation $B_{eq} = {}^8/_3 \sum_i\sum_j U_{ij} a_i^* a_j^* \mathbf{a}_i \cdot \mathbf{a}_j$. [b] The bridging hydrogen atom was refined isotropically.

Table III. Selected Bond Distances (Å) and Angles (deg) for $[Ph_4P][^2HCr_2(CO)_{10}]$

	Distances		
Cr1–Cr2	3.2465 (8)	av Cr–C_{ax}	1.833 (3)
Cr1–H	1.72 (3)	av Cr–C_{eq}	1.887 (8)
Cr2–H	1.74 (4)		
	Angles		
Cr1–H–Cr2	140 (3)	C13–Cr1–Cr2–C23	−44.3 (2)

Solid-State Deuterium NMR Spectroscopy. Deuterium powder patterns were collected at 30.709 MHz on a Bruker MSL200 solid-state NMR spectrometer. A static wideline probe was used, and ~200 mg of sample was packed into a 5-mm glass sample holder. The spectra for $[Et_4N][^2HCr_2(CO)_{10}]$ and $[Ph_4P][^2HCr_2(CO)_{10}]$ were obtained at 140, 200, and 300 K and the others only at 300 K. In order to prevent the O-ring seals about the bore tube of the superconducting magnet from freezing during the 140 K experiment, a continuous room-temperature nitrogen gas flow through the magnet bore was used. (We know of two cases where O-ring failure has lead to loss of vacuum in the Dewar and subsequent quenching of the superconducting magnet.) The spectra for $[Et_4N][^2HCr_2(CO)_{10}]$ showed some frequency shifts at lower temperatures; the spectrum acquired at 200 K exhibited an apparent isotropic

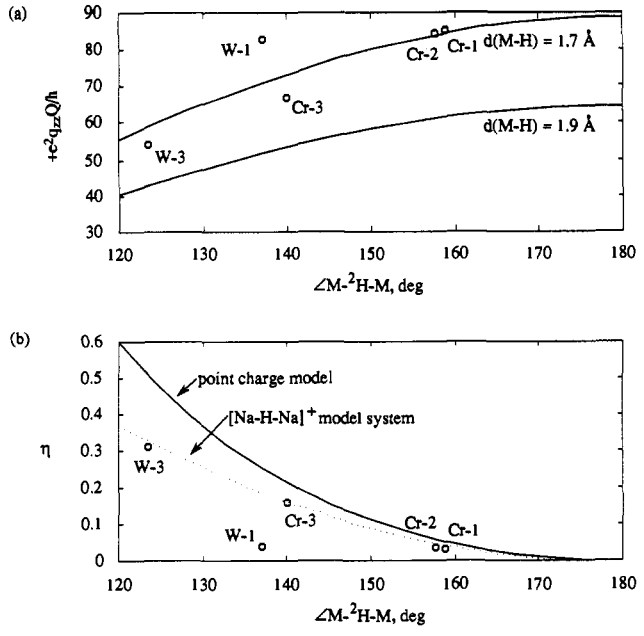

Figure 2. The effect of a nonlinear, symmetric M-^{2}H-M bond on the deuterium quadrupole coupling constant and the asymmetry parameter. (a) Two traces showing the quadrupole coupling constant as a function of M-^{2}H-M bond angle for two different M-H bond lengths. The circles (o) represent the experimental deuterium quadrupole coupling constants, and the labels are defined in Table IV. (b) The asymmetry parameter as a function of the M-^{2}H-M bond angle as computed for both a point charge model, eq 7, and an ab initio SCF-HF calculation of a model system, $[Na-H-Na]^+$ (ref 43). In the limit of a point charge representation for the metal, the value of the asymmetry parameter does not depend upon the M-H bond length.

shift of 180 ppm downfield relative to the 300 K spectrum. This shift is three times larger than the exponential line broadening and may have been due to a temperature-dependent probe magnetic susceptibility and/or a paramagnetic impurity in the sample.

The quadrupolar echo pulse sequence was used: $(90_{x,-x}-\tau_1-90_y-\tau_2-acq_{x,-x})$.[46] The 90° pulse length was 3 μs. The first delay between 90° pulses, τ_1, was 25 or 120 μs, and the second delay before echo acquisition, τ_2, was 26.5 or 121.5 μs. Delays of 120 and 121.5 μs were used only for $[(Ph_3P)_2N][^2HW_2(CO)_{10}]$ to remove a zero frequency spike possibly associated with a deuterated contaminant. A relaxation delay of 60 or 120 s was used. A two-step phase-cycling procedure, where the phase of the first 90° pulse and the receiver phase are alternated between 0° and 180°, was used in order to cancel the effects of probe ringing.[47]

Exponentially filtered (2 kHz), Fourier-transformed, and manually phased spectra were transferred as binary files from the Bruker Aspect-3000 computer to a Macintosh II computer via an RS-232 serial connection and the KERMIT file transfer program. Conversion from binary to ASCII data files was done with a program[48] written in LabVIEW, a graphical programming language.[49] Spectral simulation programs were written in Matlab, a vector-oriented programming language.[50] The Levenberg-Marquardt nonlinear least-squares algorithm[51,52] was recoded in Matlab and used in program to fit an experimental spectrum with a simulated line shape where the variables include the deuterium quadrupole coupling constant and the asymmetry parameter. The quality of the fit is judged to be good if no systematic deviations are observed in a plot of the residuals and the value of χ^2_ν is approximately one.

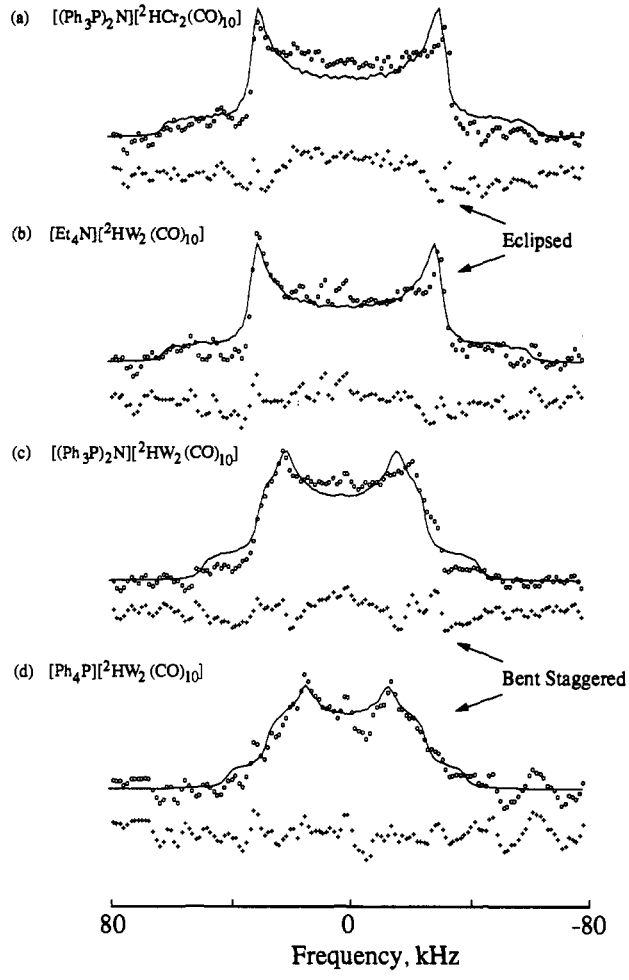

Figure 3. Solid-state deuterium NMR powder patterns obtained at 300 K for four bridging metal hydrides and the corresponding nonlinear least-squares fits. Circles (o), solid lines (-), and crosses (+) represent the experimental deuterium powder pattern, the best calculated fit, and the residual between the experimental spectrum and the fit, respectively. Experimental parameters are as follows (NS = number of scans, RD = relaxation delay): (a) $[(Ph_3P)_2N][^2HCr_2(CO)_{10}]$, NS = 6600, RD = 60 s; (b) $[Et_4N][^2HW_2(CO)_{10}]$, 3000, 120 s; (c) $[(Ph_3P)_2N][^2HW_2(CO)_{10}]$, 4360, 60 s; and (d) $[Ph_4P][^2HW_2(CO)_{10}]$, 6520, 60 s.

^{1}H CRAMPS. ^{1}H CRAMPS NMR spectra were recorded at 187 MHz on a modified Nicolet NT-200 spectrometer.[53] The BR-24 pulse sequence was utilized,[54] with pulse widths and τ values of 1.26 and 3.0 μs, respectively. Samples (ca. 50 mg) were packed into 5-mm (2 mm i.d.) NMR tubes and were spun at the magic angle at a rate of 1.5 kHz. Each spectrum was accumulated with 20 repetitions and 512 data points. Chemical shifts were measured relative to tetrakis(trimethylsilyl)methane (δ = 3.75 ppm) and are reported relative to tetramethylsilane (TMS).

Results

Figure 1b shows the X-ray crystallographic structure of the $[^2HCr_2(CO)_{10}]^-$ anion in $[Ph_4P][^2HCr_2(CO)_{10}]$. This structure is similar to, although not isomorphous with, that of the tungsten complex.[3,4] The metal carbonyl framework shows a bent staggered metal carbonyl geometry. The torsion angle defined by C13-Cr1-Cr2-C23 is -44.3 (2)°. The dihedral angle between the two planes defined by each chromium atom and the carbon atoms of its corresponding equatorial carbonyl ligands is 16.0 (4)°.

To acquire the deuterium powder patterns in these metal hydrides with acceptable signal-to-noise ratio is very difficult because of the very few deuterons in the ~200-mg sample and the quite long spin-lattice relaxation time, T_1. For example, the number

(46) Butler, L. G. *J. Magn. Reson.* **1991**, *91*, 369–9, and references therein.
(47) Fukushima, E.; Roeder, S. B. W. *Experimental Pulse NMR: A Nuts and Bolts Approach*; Addison-Wesley: Reading, MA, 1981; Chapter 5.
(48) Michaels, D. C.; Kim, A. J.; Perilloux, B. C.; Barksdale, D.; Butler, L. G. *Computers Chem.* **1991**, submitted for publication.
(49) LabVIEW for Macintosh computers, National Instruments, 6504 Bridge Point Parkway, Austin, TX 78730-5039.
(50) Matlab for VAX/VMS and Macintosh computers. The MathWorks Inc., 24 Prime Park Way, Natick, MA 01760.
(51) Bevington, P. R. *Data Reduction and Error Analysis for the Physical Sciences*; McGraw-Hill: New York, 1969.
(52) Press, W. H.; Flannery, B. P.; Teukolsky, S. A.; Vetterling, W. T. *Numerical Recipes*; Cambridge University Press: Cambridge, 1986.
(53) Bronnimann, C. E.; Hawkins, B. L.; Zhang, M.; Maciel, G. E. *Anal. Chem.* **1988**, *60*, 1743–50.
(54) Burum, D. P.; Rhim, W. K. *J. Chem. Phys.* **1979**, *70*, 3553–4.

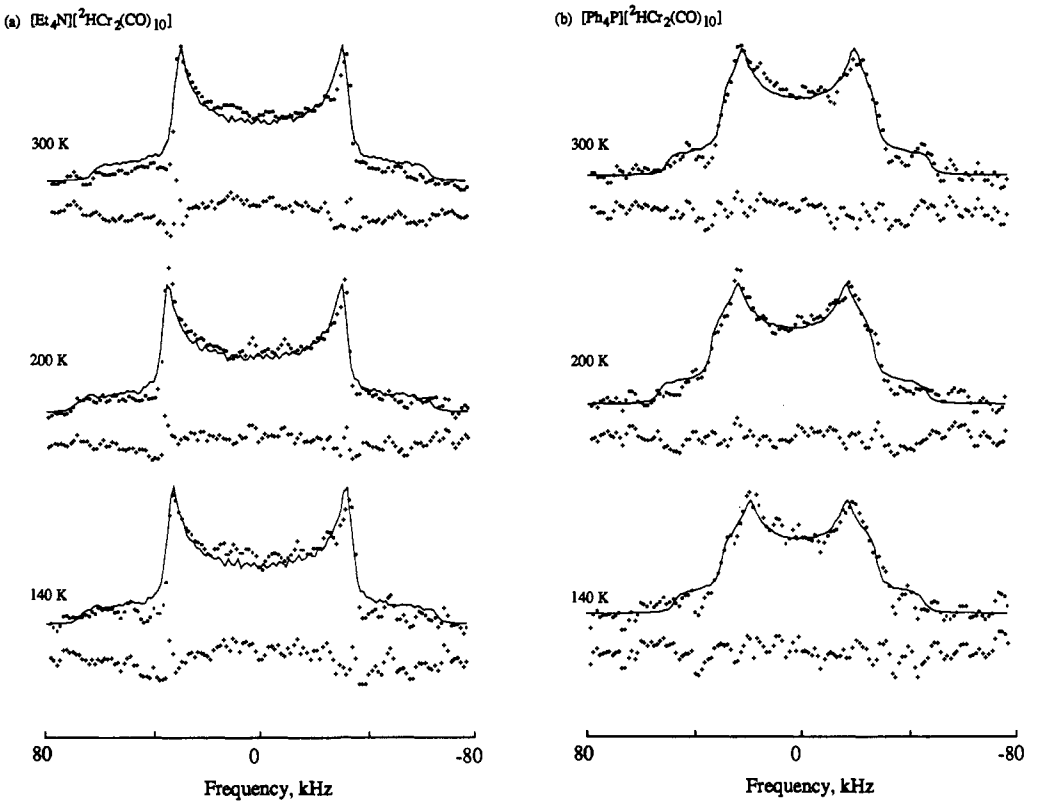

Figure 4. Solid-state deuterium NMR powder patterns obtained for two bridging metal hydrides as a function of temperature and the corresponding nonlinear least-squares fits. Experimental parameters are as follows: (a) $[Et_4N][^2HCr_2(CO)_{10}]$, T = 300 K, NS = 5730, RD = 60 s; 200 K, 500, 120 s, and 140 K, 46, 120 s and (b) $[Ph_4P][^2HCr_2(CO)_{10}]$, T = 300 K, NS = 6518, RD = 60 s; 200 K, 2150, 120 s, and 140 K, 156, 120 s.

Table IV. Deuterium Quadrupole Coupling Constants and Asymmetry Parameters, ^1H Chemical Shifts, and Crystallographic Structural Data

Fig 2 label	compd temp, K	metal–carbonyl geometry[a]	$\lvert e^2q_{zz}Q/h\rvert$, kHz	η	$\chi_\nu^{2\,b}$	chemical shift,[c] ppm	d(M–H), Å	∠(M–H–M), deg	method[d]	ref
Cr-1	$[Et_4N][^2HCr_2(CO)_{10}]$	eclipsed				−18.8	1.707 (21),	158.9 (6)	N	11
	300		85.4 (1)	0.034 (1)	2.6		1.737 (19)		(^1H, 295 K)	
	200		89.5 (2)	0.032 (3)	1.2					
	140		90.4 (2)	0.027 (3)	1.8					
Cr-2	$[(Ph_3P)_2N][^2HCr_2(CO)_{10}]$	eclipsed				−18.5	1.718 (9)–	153.9 (10)	N	14
	300		84.6 (3)	0.039 (4)	1.4		1.750 (8)	157.6 (7)	(^2H, 17 K)	
Cr-3	$[Ph_4P][^2HCr_2(CO)_{10}]$	bent staggered				NA	1.72 (3),	140 (3)	X	this work
	300		66.7 (4)	0.162 (6)	1.7		1.74 (4)		(^2H, 299 K)	
	200		68.2 (5)	0.200 (8)	1.0					
	140		63.2 (5)	0.23 (1)	1.7					
W-1	$[Et_4N][^2HW_2(CO)_{10}]$	eclipsed				−12.1	1.718 (12),	137.1 (10)	N	3, 4
	300		83.0 (4)	0.040 (4)	0.9		2.070 (12)		(^1H, 14 K)	
	$[(Ph_3P)_2N][^2HW_2(CO)_{10}]$	bent staggered				−11.6	nd[f]	nd[f]	X	15
	300		62.6 (3)	0.201 (3)	2.1				(^1H, rt[e])	
W-3	$[Ph_4P][^2HW_2(CO)_{10}]$	bent staggered				−11.1	1.897 (5)	123.4 (5)	N	4
	300		54.1 (8)	0.31 (2)	0.6				(^1H, 40 K)	

[a] See Figure 1. [b] Data variance obtained from the baseline, typically ~5%. [c] Obtained from ^1H CRAMPS results. Solution ^1H NMR chemical shifts (acetone-d_6) are $[HCr_2(CO)_{10}]^-$ salts, −19.5 ppm; $[HW_2(CO)_{10}]^-$ salts, −12.5 ppm. The chemical shift for the $[Et_4N]$ salts are in agreement with data in ref 44 for THF solution. [d] N = neutron diffraction and X = X-ray diffraction. The isotope in the bridging hydride and the temperature are also listed. [e] Room temperature = rt. [f] Not determined = nd.

of deuterons in 200 mg of $[Et_4N][^2HCr_2(CO)_{10}]$ is only 4×10^{-4} mol. The deuterium T_1 was not quantitatively measured due to the poor signal-to-noise ratio, but estimated to be 60 s or longer for $[Et_4N][^2HCr_2(CO)_{10}]$, based on spectra taken with different relaxation times. The spectra in Figure 3 required between 3000 and 6600 scans for acquisition times of 70–110 h each.

Figures 3 and 4 show the solid-state deuterium NMR powder patterns obtained at 300 K for six bridging metal hydrides and the nonlinear least-squares fits. The spectra show that three bridging deuterium sites have apparent axial symmetry, $\eta \approx 0$, and the other three do not have axial symmetry, $\eta \geq 0.16$. Because of the obvious potential for motional averaging, one compound from each group, $\eta \approx 0$ and $\eta \gg 0$, was studied as a function of temperature down to 140 K. The solid-state deuterium NMR powder patterns for $[Et_4N][^2HCr_2(CO)_{10}]$ and $[Ph_4P][^2HCr_2(CO)_{10}]$ and the nonlinear least-squares fits are shown in Figure 4 as a function of temperature. There are minor variations in the deuterium powder patterns, but no evidence for the transformation of one spectral type into the other was found. The results of the nonlinear least-squares fit to the deuterium powder patterns of all spectra are listed in Table IV.

Solid-state proton NMR spectra were collected on five of the protio complexes. The spectrum for $[Et_4N][HCr_2(CO)_{10}]$ is shown in Figure 5, and chemical shifts (relative to TMS) for the bridging hydride sites are reported in Table IV. The range of chemical shifts among the complexes of each metal is quite narrow: 0.3

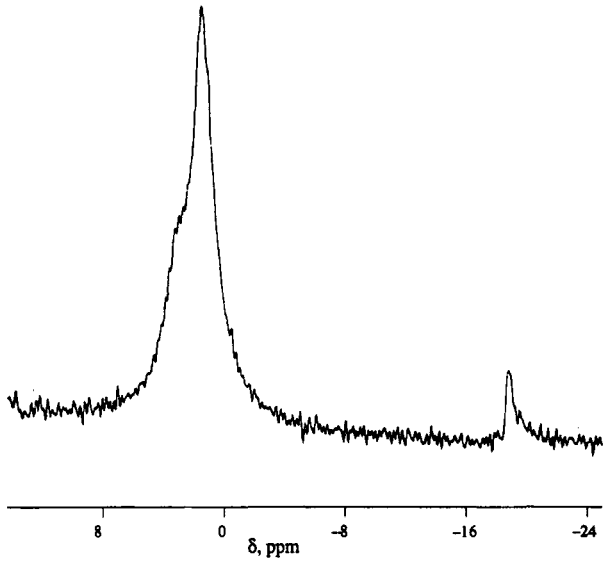

Figure 5. The ^1H CRAMPS NMR spectrum for $[Et_4N][HCr_2(CO)_{10}]$.

and 1.0 ppm for Cr and W, respectively. Inasmuch as the accuracy of the δ values obtained by the CRAMPS technique is estimated to be ±0.2 ppm, these ranges reflect insignificant chemical shift differences among complexes of the same metal and indicate that the shielding at the bridging H is quite insensitive to M–H–M geometry and metal–carbonyl conformation. Moreover, the solid-state hydride chemical shifts are nearly identical to the solution values of −19.5 and −12.5 ppm for $[HCr_2(CO)_{10}]^-$ and $[HW_2(CO)_{10}]^-$, respectively. The absence of spinning sidebands on the hydride resonances in the ^1H spectra also suggests minimal chemical shift anisotropy for these sites in the solid state.

Discussion

The interpretation of the deuterium electric field gradient parameters, the quadrupole coupling constants and the asymmetry parameters, for these bridging metal hydrides can be understood by considering three main factors: (1) the M–H bond length, (2) the M–H–M bond angle, and (3) possible rapid four-site jump motion in systems with an eclipsed metal carbonyl geometry.

The magnitude of the electric field gradient, the quadrupole coupling constant, is mainly affected by the M–^{2}H bond length since the electric field gradient has a $1/r^3$ distance dependency. From the neutron diffraction results, M–H bond distances range from 1.707 (21) to 2.070 (12) Å. To indicate this variation, two traces are shown in Figure 2a in which the value of the quadrupole coupling constant is plotted as a function of the M–H–M bond angle. The upper trace, having the larger quadrupole coupling constant, is computed using d(M–H) = 1.7 Å, whereas the lower trace represents d(M–H) = 1.9 Å. Again, the traces shown in Figure 2 are computed from a simple point charge model for a symmetric M–^{2}H–M unit. A parameter in the model, K', was determined from the experimental results for $[Et_4N][^2HCr_2(CO)_{10}]$. All deuterium sites with $|e^2q_{zz}Q/h| > 80$ kHz have at least one M–H bond length of ~1.7 Å.

To a lesser extent, the value of the quadrupole coupling constant is affected by the M–^{2}H–M bond angle. In the point charge model, the electric field gradients due to each metal add most efficiently for a bond angle of 180°. A decrease in the M–^{2}H–M bond angle causes a decrease in the value of the quadrupole coupling constant. The two metal complexes, $[Ph_4P][^2HCr_2(CO)_{10}]$ and $[Ph_4P][^2HW_2(CO)_{10}]$, have both a relatively symmetric M–H–M unit and a small M–H–M bond angle and also have the smallest quadrupole coupling constants.

The asymmetry parameter directly reflects the M–H–M bond angle, as shown in Figure 2b. As discussed earlier, the point charge model apparently exaggerates the effect of nonlinearity, so results from the study of a model system, $[Na–H–Na]^+$, obtained by ab initio molecular orbital techniques, are also shown in Figure 2b.[43] The bridging metal hydride with the most acute M–^{2}H–M bond angle, $[Ph_4P][^2HW_2(CO)_{10}]$, also has the largest asymmetry parameter, η = 0.31 (2). With the exception of the highly asymmetric $[Et_4N][^2HW_2(CO)_{10}]$ complex (d(M–H) = 1.718 (12), 2.070 (12) Å), the asymmetry parameters are extremely well fit by the $[Na–H–Na]^+$ model system. The point charge model yields an exaggerated dependence of the asymmetry parameter on the M–^{2}H–M bond angle, whereas the more diffuse charge associated with the sodium cations leads to a smaller difference between the two minor elements of the electric field gradient tensor. The largest deviation from the $[Na–H–Na]^+$ model is found for $[Et_4N][^2HW_2(CO)_{10}]$: there are two possible explanations for the deviation. First, the W–H–W unit is asymmetric[55] and has two different W–H bond lengths, thus the electric field gradient at deuterium may be similar to that of a terminal metal hydride with axial symmetry (η = 0). Second, motional effects may be important for this complex with its eclipsed metal–carbonyl geometry, as discussed below. We note here that the NMR experiment is performed at 300 K, whereas the neutron diffraction data were collected at 14 K. Therefore, the metal hydride NMR data may be affected by jump motions between hydride sites identified in the low-temperature structure.

The last factor to consider is motional averaging of the electric field gradient due to rapid jump motion of the bridging deuteron among several different sites in the M–^{2}H–M bond. In a neutron study at 17 K of $[(Ph_3P)_2N][^2HCr_2(CO)_{10}]$,[14] four equivalent off-axis sites of the bridging deuteron were refined in a system with an eclipsed metal–carbonyl geometry. Rapid jump motion among the four off-axis sites will average the two minor components, eq_{xx} and eq_{yy}, of the electric field gradient. Thus, the expected motionally averaged asymmetry parameter is zero, as may be the case here for $[Et_4N][^2HW_2(CO)_{10}]$. A near-zero asymmetry parameter indicates that the jump motion is rapid with respect to the frequency separation of the minor components of the spectrum, on the order of 10 kHz for η = 0.3 in the static limit. The $[Et_4N][^2HW_2(CO)_{10}]$ complex is an especially interesting prospect for future NMR studies at very low temperatures. Averaging the asymmetry parameter to zero would be accomplished by a four-site jump motion; a two-site jump, like that indicated in Figure 1a, would not be sufficient to change the value or orientation of the minor components.[56]

The temperature-dependent studies do not show clear evidence for rapid four-site jump motions in either complex studied. For $[Et_4N][^2HCr_2(CO)_{10}]$, which has the eclipsed structure, the fact that the asymmetry parameter remains near zero from 300 to 140 K could be interpreted as evidence that the activation barrier to a possible four-site jump motion is small (two-site rather than four-site disorder was found in the 295 K neutron diffraction study[11]). However, analysis with the point charge model suggests that even in the static limit, the asymmetry parameter for $[Et_4N][^2HCr_2(CO)_{10}]$ will be small simply as a result of the large M–^{2}H–M bond angle. Similarly, the small asymmetry parameter for $[(Ph_3P)_2N][^2HCr_2(CO)_{10}]$ may also be due to the large M–^{2}H–M bond angle rather than motional effects.

Raman and infrared spectroscopy of bridging metal hydrides is usually done at low temperature as to increase the spectral resolution for the metal–hydride stretching and bending modes.[5,57] The temperature-dependent line-broadening mechanism affecting Raman spectroscopy may also affect the deuterium electric field gradient tensor, as seen most clearly in the temperature dependence of the asymmetry parameter for $[Ph_4P][^2HCr_2(CO)_{10}]$. The sharp increase from η = 0.162 (6) at 300 K to η = 0.23 (1) at 140 K is seldom observed in NQR spectroscopy in the absence of a distinct phase change. It is not clear what the low-temperature

(55) The 17 K neutron crystallographic structural determination is made difficult because of extensive cation disorder and some disorder in the anion.

(56) The symmetry of the jump motion discussed herein differs from that of previous ^2H NMR studies. The four-site jump motion occurs between equivalent sites of a compound with D_{4h} local symmetry. The possible two-site jump motion refers to a system with local D_{2h} symmetry, in contrast to two-site jumps of phenyl rings where the effective symmetry at the deuteron is C_{2v}.

(57) Cooper, C. B.; Shriver, D. F.; Onaka, S. In *Transition Metal Hydrides*; Bau, R., Ed.; American Chemical Society: Washington, DC, 1978; pp 232–47.

limit for the asymmetry parameter might be, and further experiments are planned.

Because of crystallographic disorder, one of the complexes studied, $[(Ph_3P)_2N][^2HW_2(CO)_{10}]$, has an unknown M-H-M geometry.[15] The solid-state deuterium NMR parameters are similar to those found for $[Ph_4P][^2HW_2(CO)_{10}]$ and suggest a similar structure. Some refinement of the structural prediction is possible with the aid of the modified point charge model. The most likely M-H-M angle is more obtuse than for $[Ph_4P][^2HW_2(CO)_{10}]$, possibly about 135°, based upon the asymmetry parameter of 0.201 (3).

Conclusions

Solid-state deuterium NMR powder patterns were acquired for six bridging metal hydrides to obtain structural information on the M-^{2}H-M structure. The complexes studied have both eclipsed and bent staggered metal-carbonyl geometries. The observed deuterium powder patterns are a result of the deuterium quadrupole coupling constant, the asymmetry parameter, and, for sites with an eclipsed metal-carbonyl geometry, possible rapid four-site jump motion in the M-^{2}H-M unit. The temperature dependence of the deuterium spectrum was examined for $[Et_4N][^2HCr_2(CO)_{10}]$ and $[Ph_4P][^2HCr_2(CO)_{10}]$ which have eclipsed and bent staggered metal-carbonyl geometries, respectively. The former shows little temperature dependence beyond a slight increase in the quadrupole coupling constant. Most importantly, the apparent axial symmetry of the eclipsed metal carbonyl structure was preserved to the lowest temperature studied, 140 K, but does not necessarily indicate rapid four-site jump motion. The latter complex shows a significant increase in the asymmetry parameter, possibly correlated with the same line-broadening mechanism noted in Raman and infrared spectroscopy of the bridging metal hydrides. The deuterium quadrupole coupling constants and asymmetry parameters were related to the M-H-M bond distance and the M-H-M bond angle with a point charge model and by assuming that the sign of the quadrupole coupling constant is positive.

This work shows that solid-state deuterium NMR spectroscopy has the potential to investigate structure in metal hydrides. In particular, μ_2-bridging hydrides on surfaces should have quadrupole coupling constants and asymmetry parameters similar to those found herein for metal dimers where the important factors are the M-^{2}H bond length, the M-^{2}H-M bond angle, the effective charge on the metal, and the mobility of the deuteron across a metal surface.[58] An extension of μ_3-bridging hydrides on surfaces is possible by a change in the model presented in eq 7; briefly, the asymmetry parameter should be zero and the z-axis of the electric field gradient aligned along the C_3 axis of the triply bridging site. Otherwise, the same factors should again determine the deuterium NMR parameters.

Acknowledgment. The support of the National Science Foundation (CHE-8715517) is gratefully acknowledged. The purchase of the Bruker MSL 200 NMR spectrometer was made possible by NSF Grant CHE-8711788. Leslie G. Butler is a Fellow of the Alfred P. Sloan Foundation (1989-1991). We gratefully acknowledge Prof. J. L. Petersen for an introductory sample of $[K(crypt\text{-}222)][^2HCr_2(CO)_{10}]$. Dr. C. E. Bronnimann and the Colorado State University Regional NMR Center, funded by National Science Foundation Grant CHE-8616437, are gratefully acknowledged for providing the ^{1}H CRAMPS results.

Supplementary Material Available: Listings of bond distances and angles for $[Ph_4P][^2HCr_2(CO)_{10}]$, coordinates of hydrogen atoms, least-squares planes for the two sets of Cr-$(C_{eq})_4$ units, and anisotropic thermal parameters (7 pages); listing of observed and calculated structure factors (30 pages). Ordering information is given on any current masthead page.

(58) Kara, A.; DePristo, A. E. *J. Chem. Phys.* **1990**, *92*, 5653-60.

Evidence for Nucleophilic Addition by Muonium to Pyrazine in Water: Contrast with Ordinary Hydrogen

Zhennan Wu, Mary V. Barnabas,† John M. Stadlbauer,‡ Krishnan Venkateswaran,§ Gerald B. Porter,‖ and David C. Walker*

Contribution from the Chemistry Department and TRIUMF, University of British Columbia, Vancouver, V6T 1Y6, Canada. *Received May 1, 1991*

Abstract: The presence of heterocyclic N atoms in an aromatic solute enhance its rate of reaction toward muonium, and the free radicals formed are seen to have muonium attached to a C atom of the ring. This contrasts the behavior of ^{1}H in water, where addition to N-heterocyclic rings occurs an order of magnitude slower and with H attaching to N, at least in acid solution. Muonium evidently shows nucleophilic character while ordinary hydrogen atoms are electrophilic. Pyrazine (1,4-diazine) was used for this comparison with benzene because it has the advantage over pyridine of forming only two possible radicals.

Introduction

When H atoms in acid solution react with nitrogen heterocyclic aromatic molecules like pyrazine, free radicals are formed by addition to the ring. These radicals have been identified by ESR to result from H attaching to an N atom of the ring,[1] and the rate of reaction was reduced relative to benzene.[2] Such results were taken as an indication of the electrophilic nature of H, because N has a higher electronegativity than C, and this agrees with Hammett ρ studies with substituted benzenes.[2,3]

In the case of hydrogen's light radioactive isotope muonium (Mu), with a short-lived positive muon as its nucleus, there is evidence that electron-withdrawing groups on benzene enhance the reaction rate—suggesting Mu is nucleophilic.[4] That con-

† Present address: Chemistry Department, Argonne National Laboratory, IL 60637.
‡ Permanent address: Chemistry Department, Hood College, Frederick, MD 21701.
§ Present address: Physikalische-Chemische Institut der Universität Zürich, Switzerland.
‖ Distinguished Visiting Fellow, TRIUMF.

(1) (a) Baron, B. L.; Fraenkel, G. F. *J. Chem. Phys.* **1964**, *41*, 1455. (b) Zeldes, H.; Livingston, R. *J. Phys. Chem.* **1972**, *76*, 3348.
(2) (a) Neta, P.; Schuler, R. H. *J. Am. Chem. Soc.* **1972**, *94*, 1056. (b) Neta, P. *Chem. Rev.* **1972**, *72*, 533.
(3) Pryor, W. A.; Lin, T. H.; Stanley, J. P.; Henderson, R. W. *J. Am. Chem. Soc.* **1973**, *95*, 6993.

0002-7863/91/1513-9096$02.50/0